

Internet **Electronic** Journal of **Molecular Design**

January 2008, Volume 7, Number 1, Pages 1–11

Editor: Ovidiu Ivanciuc

Computer–Aided Drug Design of Peptide Deformylase (PDF) Inhibitors: A Docking Molecular Modeling Study

Fancui Meng,¹ Weiren Xu,² and Xian Zhao¹

¹ Institute of Crystal Materials, Shandong University, Jinan 250100, People's Republic of China

² Tianjin Institute of Pharmaceutical Research, Tianjin 300193, People's Republic of China

Received: December 5, 2007; Revised: December 20, 2007; Accepted: January 5, 2007; Published: January 31, 2008

Citation of the article:

F. Meng, W. Xu, and X. Zhao, Computer–Aided Drug Design of Peptide Deformylase (PDF) Inhibitors: A Docking Molecular Modeling Study, *Internet Electron. J. Mol. Des.* **2008**, 7, 1–11, <http://www.biochempress.com>.

Computer–Aided Drug Design of Peptide Deformylase (PDF) Inhibitors: A Docking Molecular Modeling Study

Fancui Meng,^{1,*} Weiren Xu,² and Xian Zhao¹

¹ Institute of Crystal Materials, Shandong University, Jinan 250100, People's Republic of China

² Tianjin Institute of Pharmaceutical Research, Tianjin 300193, People's Republic of China

Received: December 5, 2007; Revised: December 20, 2007; Accepted: January 5, 2007; Published: January 31, 2008

Internet Electron. J. Mol. Des. 2008, 7 (1), 1–11

Abstract

Motivation. Peptide deformylase (PDF) is essential in a variety of pathogenic bacteria but it is not required for cytoplasmic protein synthesis in eukaryotes, which makes this enzyme an attractive target for developing novel antibiotics. Because PDF inhibitors are one of the most promising classes of antibacterial agents discovered to date, we designed a series of PDF inhibitors and we predicted their biological activities using molecular simulation methods.

Method. Docking simulations of PDF inhibitors with the ligand binding pocket of PDF have been carried out. The binding conformations and binding affinities of these inhibitors have been obtained using the flexible docking protocol FlexX.

Results. Calculations performed for test compounds suggested that FlexX can reproduce the binding conformation of the crystal structure. Moreover, the predicted binding affinities have a good correlation with the biological activities of these inhibitors, thus allowing us to determine the interaction model of PDF inhibitors. A series of designed PDF inhibitors have been docked to the PDF model and the computed docking scores have been used as a reference standard to evaluate the activities of these inhibitors.

Conclusions. The results presented in this paper show that several of our designed compounds are promising PDF inhibitors.

Keywords. Peptide deformylase; PDF; inhibitors; FlexX; molecular docking; quantitative structure–activity relationships; QSAR.

Abbreviations and notations

PDF, peptide deformylase

IC₅₀, the half maximal of inhibitory concentration

QSAR, quantitative structure–activity relationships

1 INTRODUCTION

Peptide deformylase (PDF), an essential bacterial metalloenzyme, is responsible for the removal of the *N*-terminal formyl group from methionine residues following protein synthesis [1]. Because PDF is essential in a variety of pathogenic bacteria but is not required for cytoplasmic protein synthesis in eukaryotes, it is an attractive target for developing novel antibiotics [2,3] and PDF

* Correspondence author; phone: 86–531–88366330; fax: 86–531–88564464; E-mail: fancuimeng@yahoo.com.cn.

inhibitors are one of the most promising classes of antibacterial agents discovered to date. Several classes of PDF inhibitors have been reported [4–7], and among them some compounds have a pseudopeptidic scaffold [8,9] and others are β -sulfonyl and β -sulfinylhydroxamic acid derivatives [10].

As a metalloenzyme, PDF is a potential target in structure–based drug design. Using structural and mechanistic information, together with high–throughput screening, several types of potent PDF inhibitors have been identified. Most PDF inhibitors identified to date share a common structural feature of a ‘chelator + peptidomimetic’ scaffold [11]. However, there is still a need for the identification of novel and structurally diverse non–peptidic PDF inhibitors. Thus, in this paper we designed a series of PDF inhibitors and we predicted their biological activities using molecular simulation methods.

2 MATERIALS AND METHODS

2.1 Structural Models

The protein models were constructed based on the X–ray crystal structure of PDF taken from the Brookhaven Protein Data Bank, entry 1BSK [12]. The active site of PDF was defined as the collection of amino acids enclosed within an 8 Å radius sphere around Zn^{2+} . The amino acids HIS132 and HIS136 near Zn^{2+} are defined as HID (the deprotonation site is on N ϵ 2).

The ligand MLN2 has been taken from PDB 1BSK and hydrogen atoms have been added. The 3D structures of other inhibitors have been constructed using ChemOffice. MMFF94 charges have been loaded and energy minimizations have been performed. The molecular modeling and docking studies were performed on a Dell workstation using SYBYL7.0 [13].

2.2 Molecular Docking

The exponential increase in the number of protein crystal structures available from the Protein Data Bank has led to a significant interest in the direct approach to drug design, namely by directly docking a potential ligand into the active site of a receptor. FlexX is a fast, flexible docking method that uses an incremental construction algorithm to place ligands into an active site [14] and it could offer full specification of the active site, including oxidation states, metal ions, and side chain protonation states [15]. At the same time, FlexX provides reliable results for Zn^{2+} enzymes [16]. Standard parameters of the FlexX program as implemented in SYBYL 7.0 [13] were used during docking. All the flexibilities of the rotatable bonds of each inhibitor were considered in the docking process to identify the best binding conformation of the inhibitors with PDF. The scoring function (empirical binding free energy) of FlexX used to estimate the free binding energy of the protein–ligand complex was developed by Böhn and Klebe [17,18].

3 RESULTS AND DISCUSSION

3.1 Validation of the FlexX Docking Method

The ligand MLN2 of PDB 1BSK was used as a test molecule to evaluate the docking results in terms of accuracy of the predicted binding conformation in comparison with the experimental structure. MLN2 is (*s*)-2-(phosphonoxy)-caproyl-L-leucyl-*p*-nitroanilide with the structure:

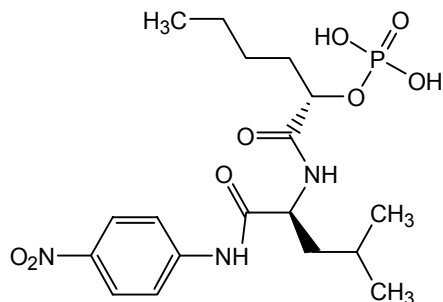


Figure 1 displays the superposition of FlexX result with the crystal structure, from which one can see that the binding conformation of MLN2 derived by FlexX docking superposes well with the crystal structure, thus demonstrating that FlexX method may predict reliable conformations of PDF inhibitors.

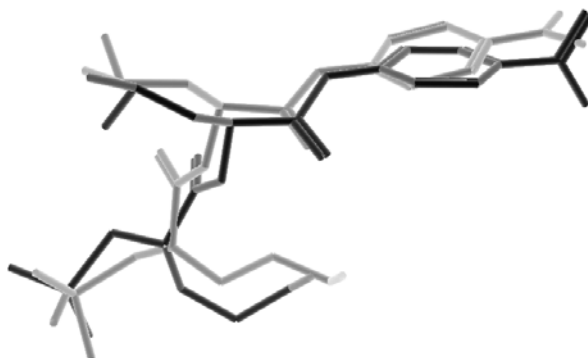


Figure 1. Superposition of the docked conformation of MLN2 (black) with that in crystallographic structure (gray).

In order to evaluate whether FlexX method could predict the binding affinity qualitatively, 56 PDF inhibitors taken from refs. [19–21] (Figure 2) have been used as test compounds. These molecules were docked into the ligand binding pocket of PDF using FlexX docking, and the docking scores and the corresponding IC_{50} values are listed in Table 1. Figure 3 shows the relationship between FlexX scores and $\log IC_{50}$. From Table 1 we could see that most compounds of group 7 have good docking scores and their corresponding IC_{50} values are low. IC_{50} s of groups 23 and 8 are larger than those of group 7. Compounds 23u, 23v and 23w were not docked into PDF and their corresponding IC_{50} are 500, 200 and 1000 respectively. Thus we can see that there exists a good correlation between FlexX docking scores and biological activities, as shown in Figure 3.

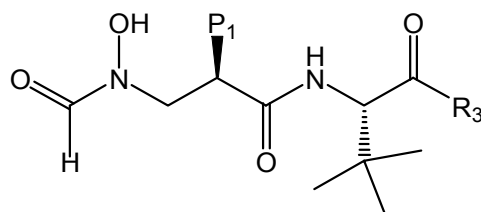


Figure 2. The structures of the test compounds of PDF inhibitors. Notes: As for **23a~23w**, R3 is $-N(CH_3)_2$, P1 is substituent; **7a~7s**, P1 is *n*-nonyl or cyclopentylmethyl, R3 is substituent; **8a~8n**, P1 is *n*-Butyl, R3 is substituent.

Table 1. Docking scores and IC_{50} values of test compounds

No.	name	score	IC_{50} (nM)	No.	name	score	IC_{50} (nM)
1	7e	-27.2	4	26	23q	-22.7	20
2	7k	-27.0	8	27	23s	-22.7	20
3	7m	-26.8	4	28	8c	-22.5	20
4	7d	-26.6	4	29	8e	-22.5	20
5	23r	-26.3	30	30	7-1	-21.9	20
6	8d	-26.3	10	31	23c	-21.6	50
7	7n	-26.2	5	32	8l	-21.6	40
8	7a	-25.9	3	33	8b	-21.4	80
9	7l	-25.7	20	34	8m	-21.3	9
10	7p	-25.7	3	35	23e	-21	10
11	7b	-25.4	3	36	8g	-20.9	10
12	7c	-25.2	5	37	23m	-20.7	20
13	7j	-25.1	8	38	8a	-20.7	30
14	7h	-24.8	1	39	8k	-20.6	30
15	7r	-24.8	7	40	23j	-20.0	10
16	23b	-24.7	70	41	7q	-20.0	3
17	8j	-24.6	20	42	8h	-20.0	10
18	7i	-24.4	3	43	7g	-19.9	8
19	23a	-24.2	100	44	8i	-19.3	10
20	8f	-24.2	50	45	23f	-18.2	30
21	BB3497	-24.1	7	46	23l	-18.2	8
22	7f	-24.0	8	47	8n	-17.6	90
23	23p	-23.9	30	48	23g	-15.8	40
24	7o	-23.8	6	49	7s	-13.8	10
25	23d	-23.4	70	50	23k	-9.7	20

Note: The structures of group **23** are taken from ref. [19], group **8** from ref. [20] and group **7** from ref. [21].

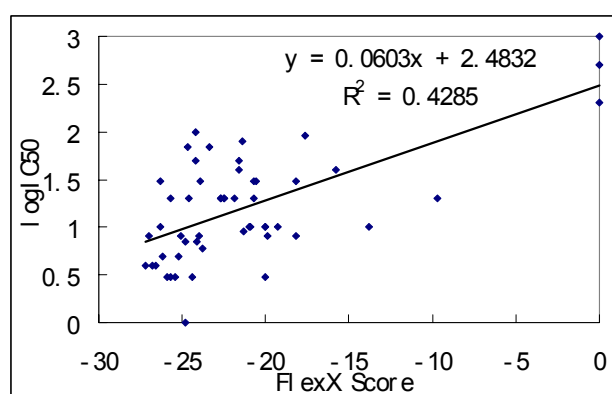
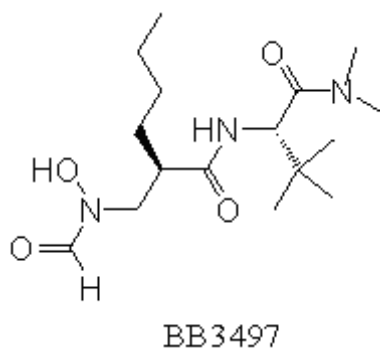


Figure 3. FlexX score vs *E. coli* PDF inhibitory activity $\log IC_{50}$.

3.2 Binding Mode of Inhibitors



Because of its simple structure for clear representation, BB3497 [22] has been used to study the binding mode of PDF inhibitors. As shown in Figure 4, BB3497 chelates to the zinc center through the *N*-formyl hydroxylamine moiety, and the carbonyl and hydroxyl oxygen atoms of the *N*-formyl hydroxylamine group act as a bidentate ligand for Zn^{2+} , and the distance between the carbonyl oxygen and Zn^{2+} is 3.34 Å whereas that between the hydroxyl oxygen atom and Zn^{2+} is 2.08 Å. BB3497 forms five hydrogen bonds with ILE44, GLN50, GLY89, LEU91 and GLU133, and its *n*-Butyl spreads to the hydrophobic cavity formed by ILE44, GLY45, LEU46, ALA47, ILE60, ASP61, VAL62, LEU125, LEU126, CYS129 and ILE130. The analysis of protein–inhibitor interactions shows that BB3497 binds well with the active cavity of PDF.

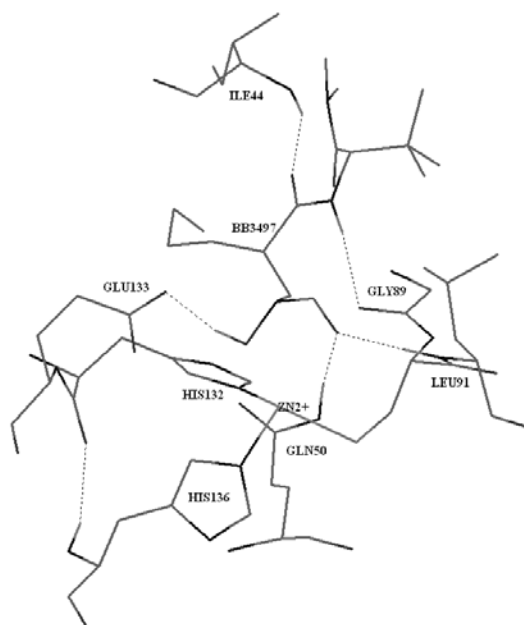


Figure 4. Hydrogen bond interaction between BB3497 and PDF (plotted using HyperChem7.0 program).

3.3 Design of PDF Inhibitors

The aforementioned PDF inhibitors involves chirality thus increases the difficulty to synthesize. In order to overcome this difficulty we change the scaffold of inhibitor to benzene or furan. The structures of our designed compounds are shown in Figure 5.

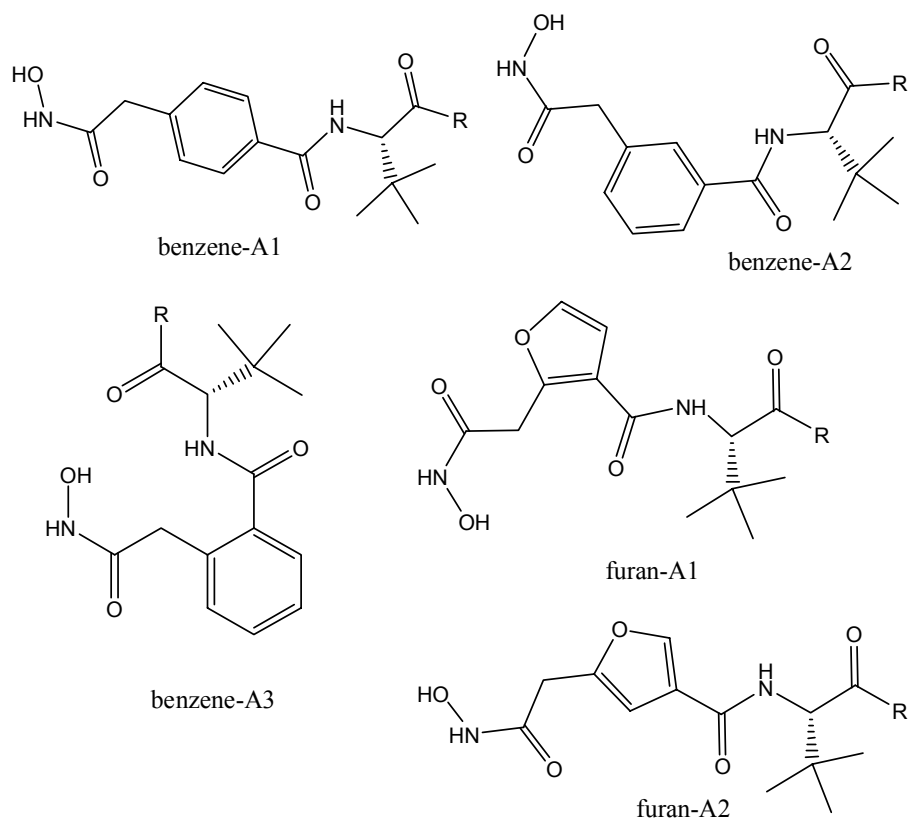


Figure 5. Structures of designed PDF inhibitors.

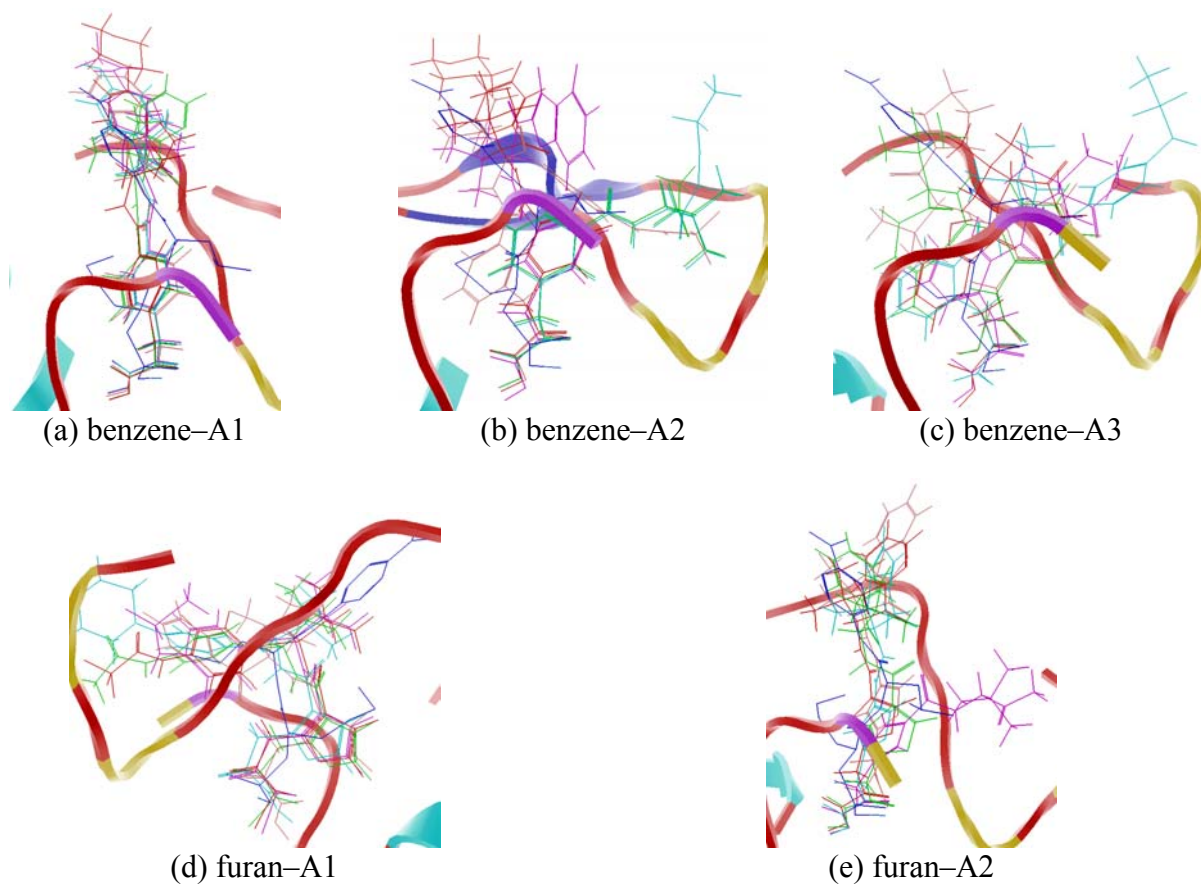


Figure 6. Superposition of the docked compounds (with the first five scores) with ligand (dark blue).

R represents the same substituents as in references [19–21]. Thus there are three databases for the benzene scaffold and two databases for the furan scaffold, denoted benzene–A1, benzene–A2, benzene–A3, furan–A1 and furan–A2, respectively. All compounds in these databases have been minimized with the MMFF94 force field and docked to PDB 1BSK using the FlexX method as in previous experiments. Comparing the data listed in Tables 2–6 with those from Table 1 we can find that the variation of the inhibitors' scaffold improves the docking scores and the most obvious one is furan–A1 whose best score amounts to –44.70. The docking scores indicate that furan–A1 obtained better results than furan–A2. As to furan–A1, the *t*-butyl is in the same direction as the benzene ring of ligand MLN2, and substituent R is in the direction of *n*-butyl of ligand MLN2. However, as to furan–A2, the superposition of the designed compounds is not good, and they also superpose poorly with ligand MLN2.

Table 2. Docking scores and predicted IC₅₀ (nM) of benzene–A1 compounds

No	Name	Score	IC ₅₀	No	Name	Score	IC ₅₀	No	Name	Score	IC ₅₀
1	M010_001	–39.40	1.28	14	M001_001	–35.00	2.36	27	M023_001	–32.10	3.53
2	M003_001	–38.70	1.41	15	M029_001	–35.00	2.36	28	M026_001	–31.90	3.63
3	M012_001	–38.50	1.45	16	M035_001	–35.00	2.36	29	M020_001	–31.80	3.68
4	M008_001	–38.30	1.49	17	M031_001	–34.90	2.39	30	M022_001	–31.50	3.83
5	M005_001	–38.20	1.51	18	M017_001	–34.20	2.64	31	M027_001	–31.40	3.89
6	M006_001	–37.60	1.64	19	M015_001	–34.00	2.71	32	M045_001	–30.60	4.35
7	M002_001	–37.10	1.76	20	M030_001	–34.00	2.71	33	M011_001	–30.10	4.66
8	M007_001	–36.60	1.89	21	M016_001	–33.60	2.86	34	M024_001	–30.00	4.72
9	M004_001	–35.90	2.08	22	M009_001	–33.50	2.91	35	M025_001	–29.90	4.79
10	M013_001	–35.70	2.14	23	M032_001	–33.50	2.91	36	M037_001	–29.80	4.86
11	M034_001	–35.40	2.23	24	M018_001	–33.40	2.95	37	M040_001	–22.00	14.34
12	M033_001	–35.30	2.26	25	M019_001	–33.20	3.03				
13	M028_001	–35.20	2.29	26	M021_001	–32.40	3.38				

Table 3. Docking scores and predicted IC₅₀ (nM) of benzene–A2 compounds

No	Name	Score	IC ₅₀	No	Name	Score	IC ₅₀	No	Name	Score	IC ₅₀
1	M005_001	–38.00	1.56	14	M002_001	–35.10	2.33	27	M022_001	–32.40	3.38
2	M001_001	–37.70	1.62	15	M007_001	–35.00	2.36	28	M029_001	–32.40	3.38
3	M012_001	–37.30	1.71	16	M009_001	–34.90	2.39	29	M026_001	–32.30	3.43
4	M030_001	–37.30	1.71	17	M028_001	–34.80	2.43	30	M033_001	–31.70	3.73
5	M010_001	–37.20	1.74	18	M013_001	–34.70	2.46	31	M037_001	–31.00	4.11
6	M006_001	–36.90	1.81	19	M020_001	–34.10	2.67	32	M036_001	–30.70	4.29
7	M016_001	–36.60	1.89	20	M008_001	–33.90	2.75	33	M024_001	–30.30	4.53
8	M023_001	–35.90	2.08	21	M014_001	–33.60	2.86	34	M039_001	–29.40	5.13
9	M031_001	–35.90	2.08	22	M015_001	–33.60	2.86	35	M043_001	–24.90	9.59
10	M019_001	–35.60	2.17	23	M025_001	–33.20	3.03	36	M045_001	–21.50	15.37
11	M018_001	–35.40	2.23	24	M004_001	–33.10	3.07	37	M011_001	–20.70	17.18
12	M003_001	–35.30	2.26	25	M021_001	–32.90	3.16	38	M041_001	–17.00	28.71
13	M017_001	–35.30	2.26	26	M027_001	–32.50	3.34				

As to the benzene scaffold compounds, benzene–A1 and benzene–A2 obtained good scoring results, but benzene–A3 is somewhat worse. The superposition maps suggest that benzene–A1 and benzene–A2 superposes well, whereas no regularities were observed for benzene–A3.

Table 4. Docking scores and predicted IC₅₀ (nM) of benzene–A3 compounds

No	Name	Score	IC ₅₀	No	Name	Score	IC ₅₀	No	Name	Score	IC ₅₀
1	M031_001	-31.80	3.68	11	M023_001	-30.10	4.66	21	M025_001	-28.00	6.23
2	M029_001	-31.70	3.73	12	M026_001	-29.90	4.79	22	M014_001	-27.80	6.41
3	M001_001	-31.50	3.83	13	M028_001	-29.60	4.99	23	M005_001	-27.70	6.50
4	M011_001	-31.50	3.83	14	M034_001	-29.60	4.99	24	M030_001	-27.40	6.78
5	M035_001	-31.40	3.89	15	M004_001	-29.40	5.13	25	M009_001	-27.10	7.06
6	M016_001	-30.90	4.17	16	M021_001	-29.40	5.13	26	M027_001	-27.10	7.06
7	M018_001	-30.90	4.17	17	M017_001	-29.00	5.43	27	M024_001	-26.50	7.68
8	M033_001	-30.40	4.47	18	M020_001	-29.00	5.43	28	M036_001	-19.40	20.58
9	M019_001	-30.30	4.53	19	M022_001	-28.40	5.90	29	M012_001	-15.70	34.39
10	M038_001	-30.30	4.53	20	M008_001	-28.30	5.98				

Table 5. Docking scores and predicted IC₅₀ (nM) of furan–A1 compounds

No	Name	Score	IC ₅₀	No	Name	Score	IC ₅₀	No	Name	Score	IC ₅₀
1	M011_001	-44.70	0.61	16	M037_001	-35.50	2.20	31	M043_001	-31.70	3.73
2	M009_001	-40.00	1.18	17	M013_001	-35.40	2.23	32	M014_001	-31.60	3.78
3	M010_001	-39.40	1.28	18	M006_001	-35.20	2.29	33	M044_001	-31.60	3.78
4	M012_001	-38.90	1.37	19	M026_001	-34.80	2.43	34	M021_001	-31.50	3.83
5	M003_001	-37.10	1.76	20	M038_001	-34.70	2.46	35	M034_001	-31.50	3.83
6	M031_001	-37.10	1.76	21	M016_001	-34.60	2.49	36	M032_001	-31.30	3.94
7	M018_001	-37.00	1.79	22	M039_001	-34.50	2.53	37	M028_001	-31.20	4.00
8	M001_001	-36.60	1.89	23	M008_001	-34.40	2.56	38	M030_001	-31.20	4.00
9	M017_001	-36.60	1.89	24	M004_001	-34.00	2.71	39	M045_001	-31.10	4.05
10	M005_001	-36.40	1.94	25	M023_001	-33.50	2.91	40	M040_001	-31.00	4.11
11	M019_001	-36.40	1.94	26	M035_001	-33.50	2.91	41	M042_001	-30.60	4.35
12	M024_001	-36.30	1.97	27	M020_001	-33.30	2.99	42	M025_001	-30.00	4.72
13	M036_001	-36.10	2.02	28	M015_001	-32.30	3.43	43	M033_001	-29.90	4.79
14	M002_001	-35.90	2.08	29	M027_001	-31.80	3.68	44	M022_001	-29.20	5.28
15	M007_001	-35.70	2.14	30	M029_001	-31.70	3.73				

Table 6. Docking scores and predicted IC₅₀ (nM) of furan–A2 compounds

No	Name	Score	IC ₅₀	No	Name	Score	IC ₅₀	No	Name	Score	IC ₅₀
1	M009_001	-36.2	2.00	16	M032_001	-32.0	3.58	31	M027_001	-27.9	6.32
2	M011_001	-36.0	2.05	17	M043_001	-31.6	3.78	32	M038_001	-27.7	6.50
3	M016_001	-35.2	2.29	18	M007_001	-31.3	3.94	33	M006_001	-27.5	6.68
4	M012_001	-34.4	2.56	19	M005_001	-30.4	4.47	34	M026_001	-27.5	6.68
5	M013_001	-34.4	2.56	20	M018_001	-30.2	4.59	35	M019_001	-27.4	6.78
6	M004_001	-34.3	2.60	21	M023_001	-30.0	4.72	36	M020_001	-27.3	6.87
7	M031_001	-34.0	2.71	22	M035_001	-29.8	4.86	37	M045_001	-27.3	6.87
8	M001_001	-33.6	2.86	23	M015_001	-29.7	4.92	38	M021_001	-26.6	7.57
9	M017_001	-33.5	2.91	24	M041_001	-29.6	4.99	39	M033_001	-24.9	9.59
10	M010_001	-33.4	2.95	25	M042_001	-29.6	4.99	40	M037_001	-24.7	9.86
11	M028_001	-33.3	2.99	26	M022_001	-29.5	5.06	41	M025_001	-24.3	10.42
12	M036_001	-32.9	3.16	27	M029_001	-29.5	5.06	42	M014_001	-8.4	94.77
13	M002_001	-32.7	3.25	28	M034_001	-29.1	5.35	43	M040_001	-7.0	115.11
14	M003_001	-32.6	3.29	29	M024_001	-28.9	5.50				
15	M030_001	-32.0	3.58	30	M008_001	-28.8	5.58				

Looking at the superposition map of benzene–A1, we also found that benzene–A1 has longer scaffold as compared with ligand MLN2, which may result in exposing the tail group and it may weaken the binding affinity of the inhibitors with PDF. Therefore, in the next part we will shorten the scaffold of these compounds to improve the binding of the inhibitors.

In a second series of experiments we decreased the scaffold of the compounds to see if the decreasing causes the binding much better than before. The carbon atoms that link *t*-butyl and the neighboring carboxyl have been removed, and the scaffold changed to be as follows:

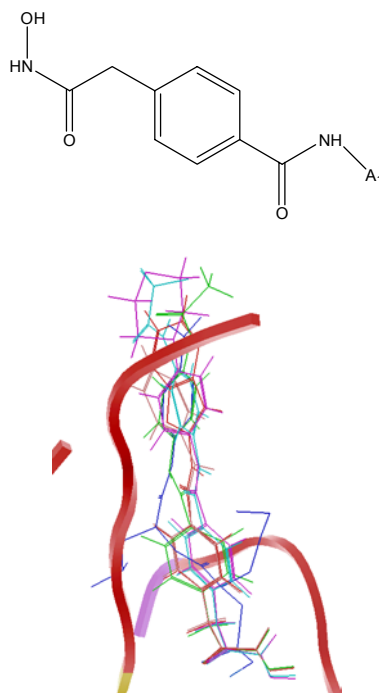


Figure 7. Superposition of benzene–A1a with ligand (dark blue).

Table 7. Docking scores and predicted IC₅₀ (nM) of benzene–A1a compounds

No	Name	Score	IC ₅₀	No	Name	Score	IC ₅₀	No	Name	Score	IC ₅₀
1	M012_001	-42.50	0.83	16	M033_001	-37.40	1.69	31	M032_001	-36.00	2.05
2	M009_001	-42.00	0.89	17	M024_001	-37.20	1.74	32	M043_001	-35.90	2.08
3	M005_001	-41.40	0.97	18	M041_001	-37.20	1.74	33	M039_001	-35.80	2.11
4	M010_001	-41.20	1.00	19	M017_001	-37.10	1.76	34	M027_001	-35.60	2.17
5	M002_001	-40.20	1.15	20	M031_001	-36.90	1.81	35	M020_001	-35.40	2.23
6	M004_001	-39.80	1.21	21	M037_001	-36.80	1.84	36	M044_001	-35.40	2.23
7	M011_001	-39.70	1.23	22	M015_001	-36.50	1.92	37	M021_001	-35.20	2.29
8	M007_001	-39.50	1.26	23	M026_001	-36.50	1.92	38	M038_001	-33.90	2.75
9	M006_001	-39.30	1.30	24	M030_001	-36.50	1.92	39	M022_001	-33.80	2.79
10	M008_001	-39.10	1.33	25	M045_001	-36.30	1.97	40	M036_001	-33.80	2.79
11	M003_001	-38.90	1.37	26	M018_001	-36.20	2.00	41	M040_001	-32.70	3.25
12	M013_001	-38.60	1.43	27	M025_001	-36.10	2.02	42	M035_001	-32.50	3.34
13	M001_001	-38.30	1.49	28	M028_001	-36.10	2.02	43	M042_001	-32.00	3.58
14	M029_001	-37.80	1.60	29	M034_001	-36.10	2.02	44	M023_001	-31.20	4.00
15	M016_001	-37.50	1.67	30	M019_001	-36.00	2.05	45	M014_001	-30.40	4.47

A1 are the same substituents as before (when the linking atom of A1 is an N atom, the NH in scaffold changes to CH₂), and the created database is named benzene–A1a. From Table 7 one can see that the docking scores improve after the scaffold shortening. The scores of the 45 compounds are all lower than -30 and the best score amounts to -42.50. At the same time, the superposition of the designed compounds with ligand MLN2 are much better than before, which indicates that the scaffold shortening of the benzene–A1 is successful.

4 CONCLUSIONS

PDF offers an attractive target for developing new antibiotics and several classes of PDF inhibitors have been discovered. With the development of computer techniques, molecular simulation plays more and more important roles in drug design, and it becomes an aid to thought and a guide to syntheses. To design potent PDF inhibitors it is important to explore the relationship between binding affinity and biological activities. Here we used the FlexX method to design a series of PDF inhibitors and we found that benzene–A1a and furan–A1 are promising PDF inhibitors. Our investigations could be used as foundation to design more effective PDF inhibitors targeted to the ligand binding pocket of PDF.

Acknowledgment

The authors acknowledge the financial of this research by China Postdoctoral Science Foundation (Grant No. 20060400991).

Supplementary Material

The structure of 1BSK used in docking (1BSK.ent) and the structures of all the 56 PDF inhibitors (inhibitor.mol2).

5 REFERENCES

- [1] J. M. Adams, On the Release of the Formyl Group from Nascent Protein, *J. Mol. Biol.* **1968**, 33, 571.
- [2] Z. Zhou, X. Song, and W. Gong, Novel Conformational States of Peptide Deformylase from Pathogenic Bacterium *Leptospira interrogans*, *J. Biol. Chem.* **2005**, 280, 42391.
- [3] C. M. Apfel, H. Locher, S. Evers, B. Takács, C. Hubschwerlen, W. Pirson, M. G. P. Page, and W. Keck, Peptide Deformylase as an Antibacterial Drug Target: Target Validation and Resistance Development, *Antimicrob. Agents Chemother.* **2001**, 45, 1058.
- [4] D. J. Durand, B. G. Green, J. F. O’Connell, and S. K. Grant, Peptide aldehyde inhibitors of bacterial peptide deformylases. *Arch. Biochem. Biophys.* **1999**, 367, 297.
- [5] Y. J. Hu, P. T. Rajagopalan, and D. Pei., H–phosphonate derivatives as novel peptide deformylase inhibitors. *Bioorg. Med. Chem. Lett.* **1998**, 8, 2479.
- [6] T. Meinel, L. Patiny, S. Ragusa, and S. Blanquet. Design and synthesis of substrate analogue inhibitors of peptide deformylase. *Biochemistry*, **1999**, 38, 4287.
- [7] J. M. Clements, R. P. Beckett, A. Brown, G. Catlin, M. Lobell, S. Palan, W. Thomas, M. Whittaker, S. Wood, S. Salama, P.J. Baker, H. F. Rodgers, V. Barynin, D. W. Rice, and M. G. Hunter, Antibiotic Activity and Characterization of BB–3497, a Novel Peptide Deformylase Inhibitor, *Antimicrob. Agents Chemother.* **2001**, 45, 563.
- [8] V. Molteni, X. He, J. Nabakka, K. Yang, A. Kreuzsch, P. Gordon, B. Bursulaya, I. Warner, T. Shin, T. Biorac, N. S. Ryder, R. Goldberg, J. Doughty, and Y. He, Identification of novel potent bicyclic peptide deformylase inhibitors, *Bioorg. Med. Chem. Lett.* **2004**, 14, 1477.
- [9] D. Z. Chen, D. V. Patel, C. J. Hackbarth, W. Wang, G. Dreyer, D. C. Young, P. S. Margolis, C. Wu, Z. J. Ni, J. Trias, R. J. White, and Z. Y. Yuan. Actinonin, a naturally occurring antibacterial agent, is a potent deformylase inhibitor. *Biochemistry* **2000**, 39, 1256.
- [10] C. Apfel, D. W. Banner, D. Bur, M. Dietz, T. Hirata, C. Hubschwerlen, H. Locher, M. G. Page, W. Pirson, G. Rosse, and J. L. Specklin. Hydroxamic acid derivatives as potent peptide deformylase inhibitors and antibacterial agents. *J. Med. Chem.* **2000**, 43, 2324.
- [11] R. Jain, A. Sundram, S. Lopez, G. Neckermann, C. Wu, C. Hackbarth, D. Chen, W. Wang, N. S. Ryder, B. Weidmann, D. Patel, J. Trias, R. White, and Z. Yuan, Substituted Hydroxamic Acids as Novel Bacterial Deformylase Inhibitor–Based Antibacterial Agents, *Bioorg. Med. Chem. Lett.* **2003**, 13, 4223.
- [12] B. Hao, W. Gong, P. T. Rajagopalan, Y. Hu, D. Pei, and M. K. Chan, Structural Basis For The Design Of Antibiotics Targeting Peptide Deformylase, *Biochemistry* **1999**, 38, 4712.

- [13] Sybyl7.0, Tripos Inc., St. Louis, MO, **2004**.
- [14] M. Rarey, B. Kramer, T. Lengauer, and G. Klebe, A Fast Flexible Docking Method using an Incremental Construction Algorithm. *J. Mol. Biol.* **1996**, 261, 470.
- [15] M. Rarey, S. Wefing, and T. Lengauer, Placement of medium-sized molecular fragments into active sites of proteins. *J. Comput.-Aided Mol. Des.* **1996**, 10, 41.
- [16] A. M. Simm, E. J. Loveridge, J. Crosby, M. B. Avison, T. R. Walsh, and P. M. Bennett, Bulgecin A: a novel inhibitor of binuclear metallo- β -lactamases, *Biochem. J.* **2005**, 387, 585.
- [17] H. J. Böhm, The development of a simple empirical scoring function to estimate the binding constant for a protein-ligand complex of known three-dimensional structure, *J. Comput.-Aided Mol. Des.* **1994**, 8, 243.
- [18] G. Klebe, The use of composite crystal-field environments in molecular recognition and the de novo design of protein ligands, *J. Mol. Biol.* **1994**, 237, 212.
- [19] S. J. Davies, A. P. Ayscough, R. P. Beckett, R. A. Bragg, J. M. Clements, S. Doel, C. Grew, S. B. Launchbury, G. M. Perkins, L. M. Pratt, H. K. Smith, Z. M. Spavold, S. W. Thomas, R. S. Todd, and M. Whittaker, Structure-Activity Relationships of the Peptide Deformylase Inhibitor BB-3497: Modification of the Methylene Spacer and the P1' Side Chain, *Bioorg. Med. Chem. Lett.* **2003**, 13, 2709.
- [20] S. J. Davies, A. P. Ayscough, R. P. Beckett, J. M. Clements, S. Doel, L. M. Pratt, Z. M. Spavold, S. W. Thomas, and M. Whittaker, Structure-Activity Relationships of the Peptide Deformylase Inhibitor BB-3497: Modification of the P2' and P3' Side Chains, *Bioorg. Med. Chem. Lett.* **2003**, 13, 2715.
- [21] S. P. East, R. P. Beckett, D. C. Brookings, J. M. Clements, S. Doel, K. Keavey, G. Pain, H. K. Smith, W. Thomas, A. J. Thompson, R. S. Todd, and M. Whittaker, Peptide deformylase inhibitors with activity against respiratory tract pathogens, *Bioorg. Med. Chem. Lett.* **2004**, 14, 59.
- [22] J. M. Clements, R. P. Beckett, A. Brown, G. Catlin, M. Lobell, S. Palan, W. Thomas, M. Whittaker, S. Wood, S. Salama, P. J. Baker, H. F. Rodgers, V. Barynin, D. W. Rice, and M. G. Hunter, Antibiotic activity and characterization of BB-3497, a novel peptide deformylase inhibitor, *Antimicrob. Agents Chemother.* **2001**, 45, 563.